Real-space local polynomial basis for solid-state electronic-structure calculations: A finite-element approach

J. E. Pask, B. M. Klein, and C. Y. Fong
Department of Physics, University of California, Davis, California 95616

P. A. Sterne
Lawrence Livermore National Laboratory, Livermore, California 94550
and Department of Physics, University of California, Davis, California 95616

(Received 2 November 1998)

We present an approach to solid-state electronic-structure calculations based on the finite-element method. In this method, the basis functions are strictly local, piecewise polynomials. Because the basis is composed of polynomials, the method is completely general and its convergence can be controlled systematically. Because the basis functions are strictly local in real space, the method allows for variable resolution in real space; produces sparse, structured matrices, enabling the effective use of iterative solution methods; and is well suited to parallel implementation. The method thus combines the significant advantages of both real-space-grid and basis-oriented approaches and so promises to be particularly well suited for large, accurate *ab initio* calculations. We develop the theory of our approach in detail, discuss advantages and disadvantages, and report initial results, including electronic band structures and details of the convergence of the method.
[S0163-1829(99)03515-8]

I. INTRODUCTION

Over the course of the last few decades, the density functional theory (DFT) of Hohenberg, Kohn, and Sham[1] has proven to be an accurate and reliable basis for the *ab initio* calculation of a wide variety of materials properties. But the solution of the Kohn-Sham equations is a formidable task, and this has significantly limited the range of physical systems which can be considered.

Among the most popular methods of solving the equations has been the plane-wave (PW) method—typically coupled with pseudopotentials to eliminate core electrons.[2] For all its advantages, however, the PW method has some notable disadvantages with respect to the solution of large problems. First, because the PW basis functions are not local in real space, they give rise to a dense Hamiltonian matrix which in turn limits the effectiveness of iterative solution methods.[3] Second, the method requires Fourier transforms which are difficult to implement efficiently on massively parallel architectures due to the need for nonlocal communications. Finally, the PW basis has the same resolution at all points in space, which causes considerable difficulties in the treatment of highly localized systems such as first-row elements and transition metals. Recent progress on this problem has included ultrasoft pseudopotentials,[4] optimized pseudopotentials,[5,6] and adaptive coordinate transformations.[7–9]

The limitations of the PW approach have inspired the development of various ''real-space'' approaches, including finite-difference (FD),[10–15] finite-element (FE),[23–26] and wavelet[29–32] methods. Of these, perhaps the most mature and successful to date have been the FD methods. These methods produce sparse, structured Hamiltonian (and in some cases, overlap) matrices, require no Fourier transforms, and allow for some degree of variable resolution in real space. But to achieve these advantages, these methods give up the use of a basis and work instead by discretizing individual terms of the equation of interest on a real-space grid. As a result, quantities of interest are defined only at a discrete set of points in space, limiting the accuracy of integrations and complicating the handling of singular functions such as all-electron potentials. And as a further consequence, the methods are not variational: the error can be of either sign and convergence is often from below.

Finite-element methods[16–28] achieve the significant advantages of FD methods without giving up the use of a basis. Like the PW method, the FE method is an expansion method. In the FE method, however, the basis functions are strictly local, piecewise polynomials. A simple one-dimensional (1D) example is shown in Fig. 1 (which we discuss further below). Because the basis is composed of polynomials, it is completely general and the convergence of the method can be controlled systematically by increasing the number or order of basis functions. Because the basis functions are strictly local in real space, the method achieves the significant advantages of FD approaches: The method produces sparse, structured matrices, which in turn enable the effective use of iterative solution methods. The method requires no Fourier transforms, as all calculations are performed in real space. And the method allows for variable resolution in real space—more so than FD approaches—by increasing the number or order of basis functions where needed. The method thus combines the significant advantages of both real-space-grid and basis-oriented approaches.

Some disadvantages of FE methods are that the matrices produced tend to be less sparse, and often less simply structured, than those produced by FD methods, and that these matrices must be stored. In addition, FE methods produce generalized rather than standard eigenvalue problems, as produced by many FD approaches, and they can be significantly

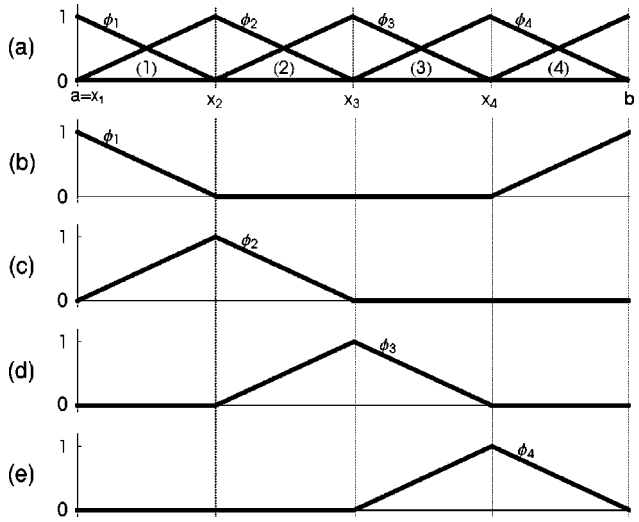

FIG. 1. Simple periodic finite-element basis: 1D, piecewise-linear case. (a) Basis. (b)–(e) Individual basis functions. The domain $[a,b]$ is partitioned into elements (subdomains) (1)–(4) within which the basis functions are simple linear polynomials. The basis is thus simultaneously polynomial and strictly local in nature.

more difficult to implement than FD or PW approaches.

The FE method[16–21] has had a long history of success in quite diverse applications ranging from civil engineering to quantum mechanics. Applications in engineering go back to the 1950s. Applications to the electronic-structure of isolated atomic and molecular systems began to appear as early as the 1970s.[22] White, Wilkins, and Teter[23] applied the method to full 3D atomic and molecular calculations in 1989 and demonstrated the advantageous scaling of the method with the number of basis functions, afforded by the strict locality and real-space nature of the basis.

There have, however, been relatively few applications to solids. Hermansson and Yevick[24] applied the FE method to full 3D solid-state electronic-structure calculations in 1986, but having reached a negative conclusion in the study of small systems with uniform meshes, discussed their approach only generally and, though apparently capable of arbitrary Brillouin zone sampling, reported only Γ-point results. More recently, Tsuchida and Tsukada[25] have applied the method to full 3D molecular and solid-state electronic-structure calculations. They have implemented self-consistency, nonuniform meshes, adaptive coordinate transformations, pseudopotential and all-electron calculations, and have demonstrated the favorable efficiency of the method relative to FD approaches. Their solid-state results have, however, also been limited to the Γ point.

Here, we present a full 3D FE approach to solid-state electronic-structure calculations which allows arbitrary sampling of the Brillouin zone, and report initial results, including electronic band structures and details of the convergence of the method. Our development differs from that of Ref. 25 in that we have taken a Galerkin approach.[27] Our development is closer to that of Ferrari,[28] who developed a Galerkin approach allowing arbitrary sampling of the Brillouin zone in the context of 2D super-lattice calculations. As we have not yet implemented self-consistency, our results here are restricted to model potentials and empirical pseudopotentials.

The remainder of the paper is organized as follows. In Sec. II we discuss the details of our approach. We begin in Sec. II A with a description of the basis. In Sec. II B we show how the basis can be applied to the solution of the Schrödinger equation subject to boundary conditions appropriate to a periodic solid. In Sec. III we present results for a model potential and Si pseudopotential, including band structures and details of the convergence of the method. The conclusions in Sec. IV are followed by an appendix giving the details of the particular 3D basis which we employ.

II. METHOD

A. Basis

Finite-element bases consist of strictly local, piecewise polynomials. They are constructed generally as follows. The domain is partitioned into subdomains called *elements*. Within each element a set of polynomial basis functions is defined. These element polynomials are then pieced together at interelement boundaries to form the piecewise polynomial basis functions of the method. In order to apply the method to periodic problems, we take the additional step here of piecing together element polynomials across the domain boundary.[33]

The essential ideas are perhaps best conveyed by a simple example: a 1D, periodic, piecewise-linear basis. Figure 1(a) shows the complete basis and Figs. 1(b)–1(e) show the individual basis functions. In this case, the domain $[a,b]$ has been partitioned into four elements. For simplicity, we have defined a uniform partition but this need not be the case in general. Within each element, two linear polynomial basis functions have been defined to make the basis complete to linear order.[34] More and higher-order polynomials can be used to increase the order of completeness. Figure 1(b) shows the basis function which results from piecing together element polynomials across the domain boundary. Figures 1(c)–1(e) show the basis functions which result from piecing together element polynomials across interelement boundaries.

Note that the resulting basis functions are C^0 continuous, i.e., continuous but not necessarily smooth.[35] Smoother bases can be constructed by requiring continuity of higher derivatives (which would require higher-order polynomials), but a C^0 basis offers a unique and potentially significant advantage: an efficient and natural representation of the wave function and charge density cusps which occur in all-electron calculations and which cause such difficulty for conventional, necessarily smooth bases—and for FD approaches as well, as they also assume some degree of derivative continuity. We have therefore chosen a C^0 basis for our approach.

The application of such a basis, however, to the solution of a second-order differential equation, with periodic boundary conditions in particular, requires some consideration. First, the application of the Laplacian to such functions is clearly problematic. Second, referring again to Fig. 1, note that the basis is value periodic, i.e.,

$$\phi_i(a^+) = \phi_i(b^-), \tag{1}$$

but not derivative periodic, i.e., it is *not* the case for all basis functions that

$$\phi_i'(a^+) = \phi_i'(b^-). \tag{2}$$

Thus, the satisfaction of periodic boundary conditions is nontrivial. We address these issues in Sec. II B.

Referring again to Fig. 1, note also that the basis functions take on a value of 1 at their associated nodes and 0 at all others, i.e.,

$$\phi_i(x_j)=\delta_{ij}. \tag{3}$$

Thus, a FE expansion

$$f(x)=\sum c_i\phi_i(x) \tag{4}$$

is such that

$$f(x_i)=c_i, \tag{5}$$

giving the expansion coefficients a direct real-space meaning.

Finally, and perhaps most significantly, we note that the basis functions are strictly local in real space, i.e., nonzero over only a (typically small) fraction of the domain. It is this property of the basis which allows the method to achieve the significant advantages of FD approaches.

In our calculations, we have employed a 3D, C^0, piecewise-cubic basis. Many other choices are possible. Higher-order completeness generally leads to smaller matrices and higher-order convergence, but also to less sparseness. The details of the particular basis which we employ are given in the Appendix.

B. Discretization

We solve

$$-\nabla^2\psi+V\psi-\varepsilon\psi=0 \tag{6}$$

in a unit cell, where V is an arbitrary periodic potential, as appropriate for a periodic solid.

We begin by reducing the Bloch-periodic problem to a periodic one. Since V is periodic, we can take ψ to be of the form

$$\psi(\mathbf{x})=u(\mathbf{x})e^{i\mathbf{k}\cdot\mathbf{x}}, \tag{7}$$

where u is a complex, cell-periodic function satisfying

$$u(\mathbf{x})=u(\mathbf{x}+\mathbf{R}) \tag{8}$$

for all lattice vectors $\mathbf{R}$. Substitution of the form (7) into Eq. (6) then gives

$$-\nabla^2u-2i\mathbf{k}\cdot\nabla u+(V+k^2-\varepsilon)u=0. \tag{9}$$

From the periodicity condition (8), we take the boundary conditions to be

$$u(\mathbf{x})=u(\mathbf{x}+\mathbf{R}_l)\quad \forall\mathbf{x}\in\Gamma_l,\quad l=1,2,3 \tag{10}$$

and

$$\hat{\mathbf{n}}\cdot\nabla u(\mathbf{x})=\hat{\mathbf{n}}\cdot\nabla u(\mathbf{x}+\mathbf{R}_l)\quad \forall\mathbf{x}\in\Gamma_l,\quad l=1,2,3, \tag{11}$$

where Γ_l and $\mathbf{R}_l$ are the surfaces of the boundary Γ and associated lattice vectors shown in Fig. 2, and $\hat{\mathbf{n}}$ is the outward unit normal at $\mathbf{x}$. We denote the domain by Ω and take it to be a parallelepiped for definiteness. The problem is thus reduced to Eqs. (9)–(11).

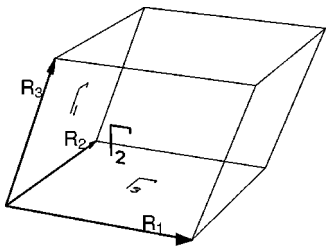

FIG. 2. Parallelepiped unit cell (domain) Ω, boundary Γ, surfaces Γ_1–Γ_3, and associated lattice vectors $\mathbf{R}_1$–$\mathbf{R}_3$.

To facilitate the use of a C^0 basis, we next derive an equivalent ''variational formulation'' of the problem. The inner product of the differential equation (9) with an arbitrary ''test function'' v gives

$$\int_\Omega v^*[-\nabla^2u-2i\mathbf{k}\cdot\nabla u+(V+k^2-\varepsilon)u]d\Omega=0. \tag{12}$$

Since v is arbitrary, the integral equation (12) is equivalent to the differential equation (9). To reduce the order of the highest derivative and produce a boundary term (whose usefulness will become clear subsequently), we integrate the ∇^2 term by parts:[36]

$$\int_\Omega\nabla v^*\cdot\nabla u d\Omega-\int_\Gamma v^*\nabla u\cdot\hat{\mathbf{n}}d\Gamma + \int_\Omega v^*[-2i\mathbf{k}\cdot\nabla u+(V+k^2-\varepsilon)u]d\Omega=0. \tag{13}$$

To incorporate the ''natural'' boundary condition (11), we now restrict v to

$$v\in\mathbf{V}=\{v:v(\mathbf{x})=v(\mathbf{x}+\mathbf{R}_l)\quad\forall\mathbf{x}\in\Gamma_l,\quad l=1,2,3\}, \tag{14}$$

i.e., to satisfy the ''essential'' boundary condition (10). Then, using the fact that the domain is a parallelepiped, the boundary term can be written as

$$\sum_l\int_{\Gamma_l}v^*(\mathbf{x})[\nabla u(\mathbf{x})-\nabla u(\mathbf{x}+\mathbf{R}_l)]\cdot\hat{\mathbf{n}}d\Gamma,$$

which vanishes upon the assertion of the natural boundary condition (11). Thus, with the restriction (14), the differential equation and natural boundary condition together imply the integral equation

$$\int_\Omega\nabla v^*\cdot\nabla u d\Omega+\int_\Omega v^*[-2i\mathbf{k}\cdot\nabla u+(V+k^2-\varepsilon)u]d\Omega=0. \tag{15}$$

Finally, using again the arbitrariness of v, it can be shown that the converse also holds, and thus that the differential formulation (9)–(11) is in fact equivalent to the following *variational formulation*: Find the scalars ε and functions $u\in\mathbf{V}$ such that

$$\int_\Omega \nabla v^* \cdot \nabla u d\Omega + \int_\Omega v^* [-2i\mathbf{k}\cdot\nabla u + (V + k^2 - \varepsilon)u] d\Omega = 0 \quad \forall v \in \mathbf{V}. \tag{16}$$

We have thus reformulated the original problem in such a way that (1) the highest derivative which occurs is of order 1 and (2) only the essential boundary condition remains—the natural boundary condition having been built into the equation itself. The problem is thus now in a form which is suitable for approximate solution in a C^0 FE basis since all terms are well defined for such functions and since such a basis can be readily constructed to satisfy the required value periodicity (e.g., Fig. 1).

To find an approximate solution, we now restrict v and u to a finite-dimensional subspace $\mathbf{V}_n \subset \mathbf{V}$. The problem is then reduced to: Find the scalars ε and functions $u \in \mathbf{V}_n$ such that

$$\int_\Omega \nabla v^* \cdot \nabla u d\Omega + \int_\Omega v^* [-2i\mathbf{k}\cdot\nabla u + (V + k^2 - \varepsilon)u] d\Omega = 0 \quad \forall v \in \mathbf{V}_n. \tag{17}$$

We proceed by constructing a real C^0 FE basis $\phi_1 \cdots \phi_n$, which satisfies the remaining essential boundary condition and so spans a subspace $\mathbf{V}_n \subset \mathbf{V}$ (e.g., Fig. 1). We then express u as a complex linear combination

$$u = \sum c_j \phi_j, \tag{18}$$

so that $u \in \mathbf{V}_n$. Substitution of the expansion (18), and the fact that Eq. (17) is satisfied $\forall v \in \mathbf{V}_n$ if it is satisfied for $v = \phi_i$, $i = 1 \cdots n$, leads finally to a generalized eigenproblem for the coefficients c_j and eigenvalues ε determining the approximate eigenfunctions and eigenvalues of the variational formulation, and thus of the original problem:

$$\mathbf{Hc} = \varepsilon \mathbf{Sc}, \tag{19}$$

where

$$H_{ij} = \int_\Omega [\nabla\phi_i \cdot \nabla\phi_j - 2i\mathbf{k}\cdot\phi_i \nabla\phi_j + (V + k^2)\phi_i\phi_j] d\Omega \tag{20}$$

and

$$S_{ij} = \int_\Omega \phi_i \phi_j d\Omega. \tag{21}$$

As in the PW method, given the expansion of the potential, the above matrix elements can be evaluated exactly, due to the polynomial nature of the basis. As in the FD method, the above matrices are sparse and structured, due to the strict locality of the basis.

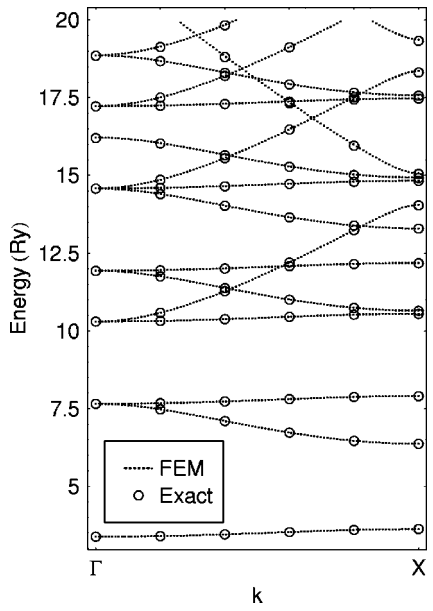

FIG. 3. FEM and exact band structures for 3D generalized Kronig-Penney potential. FEM results are for a $6\times6\times6$ uniform mesh of C^0 cubic elements. Exact results are from an analytic solution.

III. RESULTS

We have tested our approach in a number of applications ranging from the band structure of Si to positron charge distributions in C_{60}. Here we present results which demonstrate the accuracy and convergence of the method for a model potential, for which analytic results are available, and for the more physically interesting case of Si.

Figures 3 and 4 show results for a 3D generalized Kronig-Penney model potential:

$$V = V_{1D}(x) + V_{1D}(y) + V_{1D}(z), \tag{22}$$

where

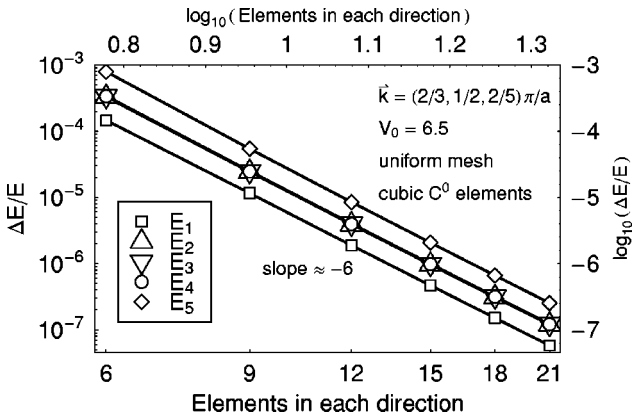

FIG. 4. Convergence of first few FEM eigenvalues for 3D generalized Kronig-Penney potential with increasing numbers of elements, at an arbitrary k point. The convergence from above demonstrates the variational nature of the method. The asymptotic slope of ≈ -6 demonstrates the sextic convergence of the method.

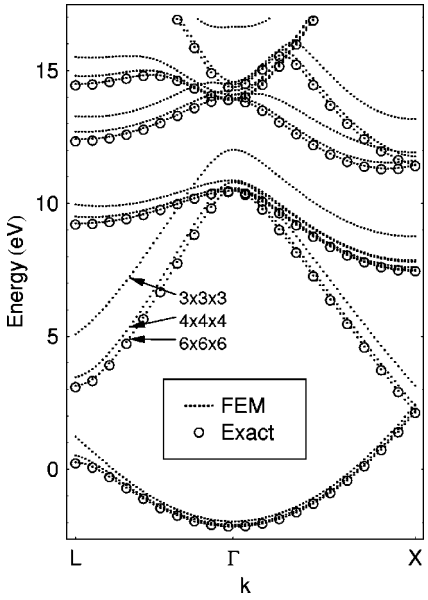

FIG. 5. FEM and exact band structures for Si pseudopotential. FEM results are for $3\times3\times3$, $4\times4\times4$, and $6\times6\times6$ uniform meshes of C^0 cubic elements. Exact results are from a highly converged plane-wave calculation. The rapid convergence and variational nature of the method are again demonstrated, with excellent agreement for the $6\times6\times6$ mesh.

$$V_{1D}(\xi)=\begin{cases}0, & 0\leqslant\xi<a\\ V_0, & a\leqslant\xi<b\end{cases}\quad\text{(periodically repeated)}. \tag{23}$$

Figure 3 shows the band structure obtained with a $6\times6\times6$ uniform mesh vs. analytic results at selected k points, for $V_0=6.5$ Ry, $a=2$ a.u., and $b=3$ a.u. More quantitative information is displayed in Fig. 4 which shows the convergence of the fractional error $(E_{\rm FEM}-E_{\rm exact})/E_{\rm exact}$ of the first few eigenvalues with increasing numbers of elements, at an arbitrary k point. The variational nature of the method is clearly demonstrated: the errors are strictly positive and monotonically decreasing. The consistent, sextic convergence of the method is also clearly demonstrated: the asymptotic slope of ≈-6 on the log-log scale corresponds

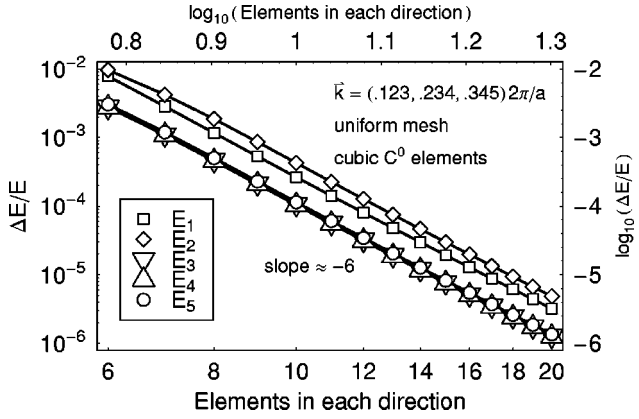

FIG. 6. Convergence of first few FEM eigenvalues for Si pseudopotential with increasing numbers of elements, at an arbitrary k point. The variational nature and consistent, sextic convergence of the method are again demonstrated.

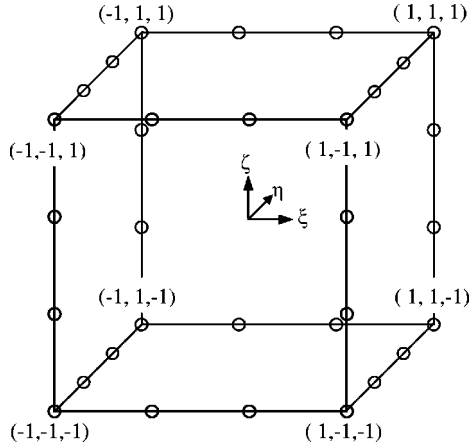

FIG. 7. Three-dimensional C^0 cubic parent element and associated nodal positions (denoted by open circles).

to an error of $O(h^6)$, where h is the mesh spacing, consistent with FE asymptotic convergence theorems for the cubic-complete case.[37]

Figures 5 and 6 show results for a Si pseudopotential.[38] Since our approach allows for the direct treatment of an arbitrary parallelepiped domain, we show results for a two-atom primitive cell. In contrast, recent FD approaches have been limited to a small subset of Bravais lattices and have reported only supercell results for Si. Figure 5 shows the sequence of band structures obtained for $3\times3\times3$, $4\times4\times4$, and $6\times6\times6$ uniform meshes vs exact values at selected k points. (Here ''exact values'' are from a highly converged PW calculation, using a 54 Ry cutoff.) The variational nature and rapid convergence of the method are again clearly demonstrated. Also apparent in the very coarse $3\times3\times3$ results, are the inexact degeneracies of certain eigenvalues at high-symmetry k points: for example, the splitting at the Γ point of the triply degenerate value at the top of the valence band and the splitting at the X point of the doubly degenerate lowest value. As noted in Ref. 24, this is due to the fact that the basis is not constrained to have the full symmetry of the crystal. Thus, to the extent that the eigenvalues are approximate, so are the degeneracies; and as the eigenvalues converge, the degeneracies become exact. By the $6\times6\times6$ mesh, the splittings are no longer apparent. Figure 6 shows the convergence of the fractional error of the first few eigenvalues with increasing numbers of elements, at an arbitrary k point. The variational nature and consistent, sextic convergence of the method are again clearly demonstrated.

IV. SUMMARY AND CONCLUSIONS

We have presented an approach to solid-state electronic-structure calculations based on the finite-element method. In Sec. II A we discussed the details of the basis, the most important being its polynomial composition and strict locality, leading to its generality and suitability for large-scale calculations. In Sec. II B we developed our approach to the solution of the Schrödinger equation, subject to boundary conditions appropriate to a periodic solid, using a C^0 finite-element basis: yielding a general method for solid-state electronic-structure calculations, allowing arbitrary sampling of the Brillouin zone. In Sec. III we presented initial results

illustrating the accuracy and convergence of the method in electronic band-structure calculations. The consistent, sextic convergence and variational nature of the method were demonstrated.

The finite-element method combines the significant advantages of both real-space-grid and basis-oriented approaches and so promises to be particularly well suited for large, accurate *ab initio* calculations. The results to date are promising, but the application of the finite-element method to solid-state electronic-structure calculations is still in its infancy and whether it will ultimately prove superior to other approaches will only be known after much further development. Our approach has already proven effective in large (863 atoms), non-self-consistent positron distribution and lifetime calculations.[39] Work on the addition of self-consistency, optimization of numerical methods, and parallelization is underway.

ACKNOWLEDGMENTS

J.E.P. would like to thank N.A. Modine, J.-L. Fattebert, F. Gygi, and D.C. Sorensen for helpful discussions and/or guidance concerning numerical methods and G.L.W. Hart and M.C. Fallis for helpful discussions throughout the course of this work. Support for this work from the University of California Campus–Laboratory Collaboration Program is gratefully acknowledged. This work was performed, in part, under the auspices of the U.S. Department of Energy by Lawrence Livermore National Laboratory under Contract No. W-7405-ENG-48.

APPENDIX

In this appendix we discuss the details of the 3D FE basis used in this work. We have employed standard 3D 32-node ''serendipity'' elements.[40] These afford C^0 flexibility and cubic completeness with a minimum number of basis functions per element. As in standard FE references, we list below the *parent basis functions* defined on the *parent element*: $[-1,1]^3$. The basis functions associated with any particular element are derived from these by a transformation.[41] This permits the construction of quite general element meshes, permitting the precise concentration of degrees of freedom in real space where needed. For simplicity, we have limited our implementation to affine transformations. These are general enough to permit the direct treatment of an arbitrary parallelepiped domain and thus of any Bravais lattice.

The parent element and associated nodal positions (denoted by open circles) are shown in Fig. 7. The 32 parent basis functions ϕ_i and associated nodes (ξ_i,η_i,ζ_i) are listed below:

(ξ_i,η_i,ζ_i)	ϕ_i
$(\pm 1,\pm 1,\pm 1)$	$\frac{1}{64}(1+\xi_0)(1+\eta_0)(1+\zeta_0)\{9(\xi^2+\eta^2+\zeta^2)-19\}$
$(\pm \frac{1}{3},\pm 1,\pm 1)$	$\frac{9}{64}(1-\xi^2)(1+9\xi_0)(1+\eta_0)(1+\zeta_0)$
$(\pm 1,\pm \frac{1}{3},\pm 1)$	$\frac{9}{64}(1-\eta^2)(1+9\eta_0)(1+\xi_0)(1+\zeta_0)$
$(\pm 1,\pm 1,\pm \frac{1}{3})$	$\frac{9}{64}(1-\zeta^2)(1+9\zeta_0)(1+\xi_0)(1+\eta_0)$

where

$$\xi_0=\xi_i\xi, \quad \eta_0=\eta_i\eta, \quad \zeta_0=\zeta_i\zeta.$$

Thus, for example, the parent basis function associated with the node $(-\frac{1}{3},1,1)$ is $\frac{9}{64}(1-\xi^2)(1-3\xi)(1+\eta)(1+\zeta)$; the one associated with the node $(-1,\frac{1}{3},1)$ is $\frac{9}{64}(1-\eta^2)(1+3\eta)(1-\xi)(1+\zeta)$, etc. Each takes on a value of 1 at its associated node and 0 at all others.

Upon piecing together element basis functions across interelement and domain boundaries, the resulting periodic piecewise-cubic basis contains seven basis functions per element.

[1] P. Hohenberg and W. Kohn, Phys. Rev. **136**, B864 (1964); W. Kohn and L.J. Sham, *ibid.* **140**, A1133 (1965).

[2] See, e.g., W.E. Pickett, Comput. Phys. Rep. **9**, 115 (1989) for a comprehensive review.

[3] Matrix-vector multiplies—the central operations in iterative solution methods—scale at best as $N\log N$, as compared to N for sparse matrices, where N is the dimension of the matrices.

[4] D. Vanderbilt, Phys. Rev. B **41**, 7892 (1990); K. Laasonen, R. Car, C. Lee, and D. Vanderbilt, *ibid.* **43**, 6796 (1991).

[5] A.M. Rappe, K.M. Rabe, E. Kaxiras, and J.D. Joannopoulos, Phys. Rev. B **41**, 1227 (1990).

[6] J.S. Lin, A. Qteish, M.C. Payne, and V. Heine, Phys. Rev. B **47**, 4174 (1993).

[7] F. Gygi, Europhys. Lett. **19**, 617 (1992); Phys. Rev. B **48**, 11 692 (1993); **51**, 11 190 (1995).

[8] A. Devenyi, K. Cho, T.A. Arias, and J.D. Joannopoulos, Phys. Rev. B **49**, 13 373 (1994).

[9] D.R. Hamann, Phys. Rev. B **51**, 7337 (1995); **51**, 9508 (1995); **56**, 14 979 (1997).

[10] J.R. Chelikowsky, N. Troullier, and Y. Saad, Phys. Rev. Lett. **72**, 1240 (1994); J.R. Chelikowsky, N. Troullier, K. Wu, and Y. Saad, Phys. Rev. B **50**, 11 355 (1994); J.R. Chelikowsky, *ibid.* **57**, 3333 (1998).

[11] E.L. Briggs, D.J. Sullivan, and J. Bernholc, Phys. Rev. B **52**, R5471 (1995); **54**, 14 362 (1996); J. Bernholc, E.L. Briggs, D.J. Sullivan, C.J. Brabec, M. Buongiorno Nardelli, K. Rapcewicz, C. Roland, and M. Wensell, Int. J. Quantum Chem. **65**, 531 (1997).

[12] G. Zumbach, N.A. Modine, and E. Kaxiras, Solid State Commun. **99**, 57 (1996); N.A. Modine, G. Zumbach, and E. Kaxiras, Phys. Rev. B **55**, 10 289 (1997).

[13] F. Gygi and G. Galli, Phys. Rev. B **52**, R2229 (1995).

[14] K.A. Iyer, M.P. Merrick, and T.L. Beck, J. Chem. Phys. **103**, 227 (1995); T.L. Beck, K.A. Iyer, and M.P. Merrick, Int. J. Quantum Chem. **61**, 341 (1997); T.L. Beck, *ibid.* **65**, 477 (1997).

[15] T. Hoshi, M. Arai, and T. Fujiwara, Phys. Rev. B **52**, R5459 (1995).

[16] D.S. Burnett, *Finite Element Analysis* (Addison-Wesley, Reading, MA, 1987).

[17] O.C. Zienkiewicz and R.L. Taylor, *The Finite Element Method*,

4th ed. (McGraw-Hill, London, 1988).
[18] K.-J. Bathe, *Finite Element Procedures* (Prentice Hall, Englewood Cliffs, NJ, 1996).
[19] G. Strang and G.J. Fix, *An Analysis of the Finite Element Method* (Prentice-Hall, Englewood Cliffs, NJ, 1973).
[20] K. Eriksson, D. Estep, P. Hansbo, and C. Johnson, *Computational Differential Equations* (Cambridge University Press, Cambridge, 1996).
[21] B.D. Reddy, *Introductory Functional Analysis* (Springer-Verlag, New York, 1998).
[22] For a review, see J. Linderberg, Comput. Phys. Rep. **6**, 209 (1987); J.J.S. Neto and J. Linderberg, Comput. Phys. Commun. **66**, 55 (1991).
[23] S.R. White, J.W. Wilkins, and M.P. Teter, Phys. Rev. B **39**, 5819 (1989).
[24] B. Hermansson and D. Yevick, Phys. Rev. B **33**, 7241 (1986).
[25] E. Tsuchida and M. Tsukada, Solid State Commun. **94**, 5 (1995); Phys. Rev. B **52**, 5573 (1995); **54**, 7602 (1996).
[26] J.E. Pask, B.M. Klein, and C.Y. Fong, Bull. Am. Phys. Soc. **43**, 40 (1998).
[27] See, e.g., Ref. 16.
[28] R.L. Ferrari, Int. J. Numer. Modelling: Electronic Networks, Devices and Fields **6**, 283 (1993).
[29] K. Cho, T.A. Arias, J.D. Joannopoulos, and P.K. Lam, Phys. Rev. Lett. **71**, 1808 (1993).
[30] S. Wei and M.Y. Chou, Phys. Rev. Lett. **76**, 2650 (1996).
[31] C.J. Tymczak and X.Q. Wang, Phys. Rev. Lett. **78**, 3654 (1997).
[32] R.A. Lippert, T.A. Arias, and A. Edelman, J. Comput. Phys. **140**, 278 (1998).
[33] For details see, e.g., Ref. 21, Chap. 11; Ref. 16, Chaps. 5 and 13. The details of the additional step of piecing together across the domain boundary then follow straightforwardly from Sec. II.
[34] A polynomial basis which is complete to order n spans the space of polynomials of order n.
[35] A function is of class C^n if the function and its first n derivatives are continuous.
[36] We assume that v is sufficiently well behaved to keep the integrals well defined. For details regarding the relevant function spaces, see, e.g., Refs. 19 and 21.
[37] See e.g., Ref. 16, p. 426.
[38] M.L. Cohen and T.K. Bergstresser, Phys. Rev. **141**, 789 (1966).
[39] P.A. Sterne, J.E. Pask, and B.M. Klein, Appl. Surf. Sci. (to be published).
[40] See, e.g., *Finite Element Handbook*, edited by H. Kardestuncer *et al.* (McGraw-Hill, New York, 1987), p. 2.126.
[41] This is among the most common methods of generating FE bases. For details, see, e.g., Ref. 16, Chaps. 8 and 13.